Gravity and Wind Load Path Analysis of a Light-Frame and a Traditional Timber Frame Building

Brian P. Malone, S.M.ASCE[1]; Thomas H. Miller, M.ASCE[2]; and Rakesh Gupta, M.ASCE[3]

Abstract: The objective of this study was to compare structural load path and system behavior of a light-frame (LF) and a timber frame (TF) structure. This load path analysis is part of a broader research effort that compares LF to TF residential structures. Structural analysis software was used to create a model of each structure. The TF structure was composed of large-dimension timbers and structural insulated panels (SIPs). An equivalent LF structure was designed for comparison, following the guidelines of the International Residential Code. Results show that TF outperforms LF in resisting uplift, as well as in story drift. TF also provides load paths that are more resistant to the introduction of large openings and the loss of a central post. Observed axial loads in TF posts show smaller ranges compared with LF studs. **DOI: 10.1061/(ASCE)AE.1943-5568.0000136.** © 2013 American Society of Civil Engineers.

Author keywords: Wood structures; Timber construction; Structural behavior.

Introduction

Investigations on structural load path and system behavior of light-frame (LF) wooden structural systems have been performed in the wake of poor performance of these buildings when subject to extreme weather events (such as hurricanes and tornadoes) (van de Lindt et al. 2007; Prevatt et al. 2012). Recent studies have involved the development of modeling techniques based on experimental results from partial or full-scale testing (Doudak 2005; Martin et al. 2011; Pfretzschner et al. 2013). Wood LF structures comprise the majority of residential structures in the United States (Allen and Thallon 2011), yet have proven to be particularly vulnerable to high wind–induced damage (van de Lindt et al. 2007). Where there is room to improve, computer modeling of these structures can aid designers and builders in predicting performance and therefore in making more informed design decisions.

Before the introduction of light-framing practices, wood frames were constructed from large-dimension timber, connected by mortise-and-tenon-style joinery, and fastened with wooden pins, a structural system known as a timber frame (TF). Today, timber framing has evolved from its traditional roots to offer a modern product, an alternative to light framing that is worth investigating with respect to structural performance. In an industry where safety of inhabitants is of utmost concern and improvements are necessary, comparison of available structural systems can highlight the strengths and weaknesses of different structural systems for the application of this knowledge to future design and structural system selection. Although qualitative reasoning to evaluate the structural characteristics of each

is valid for some decisions, a quantitative analysis of performance is the only way to arrive at conclusive results and make truly informed decisions. Structural analysis of each is necessary, and creation of models with structural analysis software makes this possible during the design stage. Research efforts to model traditional TF structural performance have primarily focused on the behavior of mortise-and-tenon joints (Erikson and Schmidt 2003; Shanks and Walker 2009; Bulleit et al. 1999). Structural modeling of whole-system TFs, however, has not been performed and presented in the literature as for LFs. Furthermore, no modeling method has been applied to both structural systems for direct comparison.

Objectives

The main objective of this study was to create practical structural analysis models of TF and LF for structural behavior and load path comparison. The two separate, complete structural systems are compared with the most commonly used building components in each construction technique. Comparisons are made between the TF structure and the LF structure with respect to uplift, story drift, the introduction of large openings, a break in load path, and range of axial loading in vertical members (posts and studs).

Methods and Materials

Structural System Design

Timber Frame
The TF structure designed for this study was based on an existing TF building. This building was completed in 2011 in Jay, Vermont, and served as the inspiration for this study. Structural design of this TF structure was verified with the National Design Specification (NDS) [American Forest and Paper Association (AF&PA) 2005a], and member size was dictated largely by the size necessary to facilitate mortise-and-tenon-style joinery. Calculations show that some members, such as posts, are overconservative, whereas others, such as rafters, are adequate.

The Vermont structure was constructed of solid-sawn, unseasoned (green) eastern hemlock (*Tsuga canadensis*) timbers by traditional timber framing methods. All joinery was mortise-and-tenon-style, fastened primarily with wooden pins. The TF structure for this study

[1]Graduate Research Assistant, School of Civil and Construction Engineering and Dept. of Wood Science and Engineering, Oregon State Univ., Corvallis, OR 97331. E-mail: malonebp@gmail.com

[2]Associate Professor, School of Civil and Construction Engineering, Oregon State Univ., Corvallis, OR 97331 (corresponding author). E-mail: thomas.miller@oregonstate.edu

[3]Professor, Dept. of Wood Science and Engineering, Oregon State Univ., Corvallis, OR 97331. E-mail: rakesh.gupta@oregonstate.edu

was designed using the NDS (AF&PA 2005a) and follows the guidelines outlined by the "Standard for Design of Timber Frame Structures" [TF Engineering Council (TFEC) 2010]. See Malone (2013) for a thorough description of the design of this structure.

Although the Vermont structure is sheathed with solid-sawn materials, the model created for this study is sheathed with structural insulated panels (SIPs) because of their current popularity in industry. Fig. 1 shows a rendering (*Google Sketch-Up Pro 8.0.15158*) of this structure shown without SIPs (for clarity).

The structural systems designed for this study reflect a rectangular 2-story residential building that has a 7.9×12.2-m (26×40-ft) footprint, is approximately 8.0 m (26.5 ft) high at the gable, and has a 9:12-slope gable roof. The bottom story has two garage doors on one gable end and a person door on one side. There are three windows on the first story and eight on the second. This building is located in the town of Jay, Vermont, and design loads are based on requirements for this location.

Light Frame

An equivalent LF structure was designed based on the modified Vermont TF structure. Equivalence for this design was defined as maintaining building envelope and shape and meeting the same operational needs as the modified TF structure. Structures designed for this study reflect a typical design for each framing method, and therefore equivalence was not based on structural capacity. This structure is framed with spruce-pine-fir (SPF) dimensional lumber with 38×140-mm (2×6-in.) walls and sheathed with plywood. Design of the LF was performed in accordance with the prescriptive guidelines outlined in the 2009 International Residential Code (IRC) [International Code Council (ICC) 2009]. Where design requirements could not be met by these guidelines, necessary components of the structural system were engineered according to the NDS (AF&PA 2005a). These components include the beams that support the floor and the columns that centrally support these beams. Additionally, where available shear wall area on the gable end with garage door openings was deemed insufficient by the IRC for lateral force resistance, a moment-resisting portal frame was engineered following the guidelines published by Martin et al. (2008). Fig. 1 shows a rendering (*Google Sketch-Up Pro*) of the TF and LF structures designed for modeling in this study.

Design Loading

Design loads applied to each structure included dead, live, snow, and wind loads and were assigned based on the location of the Jay, Vermont,

structure. Dead loads were assigned using material properties (weights) for frame and shell elements and were based on species and product type. Panel product [oriented strand board (OSB) and plywood] specific gravities (SGs) were provided by the APA Panel Design Specification (APA Engineered Wood Association 2012), and solid-sawn material densities were based on the SG on an oven-dry (OD) basis of species selected (to conservatively estimate the weights of members), and were provided by the NDS (AF&PA 2005a). Live, wind, and snow loads were applied directly to appropriate sheathing elements within the model, and lateral (wind) loads were considered from both general directions. Each general wind direction refers to a range of wind angles. Live loads applied to the floor of each structure were determined with ASCE 7-10 (ASCE 2010). Similarly, ASCE 7-10 was used to calculate wind loading. Wind pressures were determined using the simplified envelope procedure for low-rise buildings as outlined in part 2 of chapter 28 of ASCE 7-10 (ASCE 2010). For a detailed description of these wind loading calculations, see Malone (2013). Design snow loads were dictated by the town of Jay, Vermont.

Table 1 is an overview of all load applied to the structures. Fig. 2 indicates calculated wind load assignments (wind pressures) from the general east-west and north-south directions (ASCE 2010).

Allowable stress design (ASD) load combinations 4, 5, and 6a (ASCE 2010), indicated in Eqs. (1), (2), and (3), were chosen for the application of design loads to each structure.

$$\text{Load combination 4: } D + 0.75L + 0.75S \qquad (1)$$

$$\text{Load combination 5: } D + 0.6W \qquad (2)$$

$$\text{Load combination 6a: } D + 0.75L + 0.75(0.6W) + 0.75S \qquad (3)$$

where D = dead load; L = live load; S = snow load; and W = wind load.

These load combinations were used to observe load path and system behavior based on gravity loads only, loading considering the effects of wind and 100% of dead load only, and from the interaction of all applicable loads, respectively. Where openings did not allow direct application of these loads to sheathing, their equivalent effects on door and window framing were calculated and applied as appropriately distributed loads to these framing elements.

Modeling Methods

Modeling methods developed by Martin et al. (2011) and further developed and validated by Pfretzschner et al. (2013) were used for
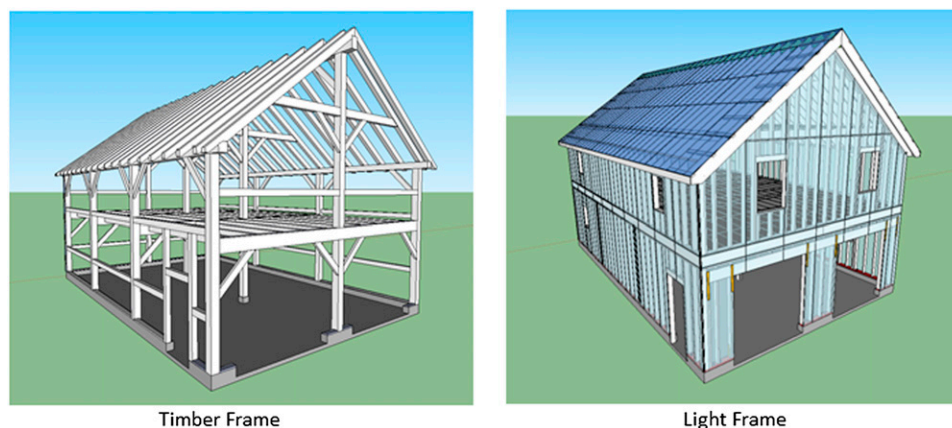

Fig. 1. TF design (without SIPs) and LF design

Table 1. Load Assignments for Structures Studied

Loading	Application	Magnitude	Unit	Based on	Source
Dead	SPF framing	420 (26.2)	kg/m^3 (lb/ft^3)	SG = 0.42 (OD)	NDS (AF&PA 2005a)
	Eastern hemlock framing	420 (26.2)	kg/m^3 (lb/ft^3)	SG = 0.42 (OD)	NDS (AF&PA 2005a)
	Plywood	420 (26.2)	kg/m^3 (lb/ft^3)	SG = 0.42 (OD)	Panel Design Specification (APA Engineered Wood Association 2012)
	OSB	500 (31.2)	kg/m^3 (lb/ft^3)	SG = 0.50 (OD)	Panel Design Specification (APA Engineered Wood Association 2012)
Live	Floor sheathing	195 (40)	kg/m^2 (lb/ft^2)	Residential	ASCE 7-10 (ASCE 2010)
Wind	Wall and roof sheathing	Varies	kg/m^2 (lb/ft^2)	Simplified envelope method	ASCE 7-10 (ASCE 2010)
Snow	Roof sheathing	293 (60)	kg/m^2 (la/ft^2)	Local requirements	Town of Jay, Vermont

the creation of structural models. These methods were developed using *SAP2000* software, and therefore all models in this study were created with this commercially available program (Computers and Structures 2012). Both the TF and the LF structures were modeled with and without openings (doors, windows), referred to as standard and enclosed, respectively. Fig. 3 shows the LF structure model, depicted both completely enclosed and with openings (standard), as well as similar images of the TF structure.

Framing Members
Framing members were modeled according to methods developed by Martin et al. (2011) and Pfretzschner et al. (2013). Framing members for both TF and LF were modeled using *SAP2000*'s frame element (Computers and Structures 2012). Framing elements of all sizes, 38×140-mm (2×6-in.) LF studs and 203×203-mm (8×8-in.) TF posts alike, were modeled similarly and assigned isotropic material properties. An alternate approach would have been to use transversely isotropic properties rather than the actual orthotropic material properties for these members. Multiple members framed longitudinally adjacent in the LF, such as a double top plate or a built-up post, were modeled using a single framing element with a cross section as the sum of the individual cross sections. Isotropic material properties for framing members were assigned based on the NDS (AF&PA 2005a) and species and grade selection. LF members were No. 1/2 SPF and TF members were No. 1 eastern hemlock.

Sheathing
Sheathing was also modeled according to methods developed by Martin et al. (2011) and Pfretzschner et al. (2013). Wall sheathing was modeled using *SAP2000*'s layered shell element as one continuous shell element applied to each wall, floor, or roof. Each shell element was then meshed into approximately 203×203-mm (8×8-in.) sections. Wall shell elements were modeled through the center of wall framing members (LF studs or TF posts) and assigned an offset from this center line to the appropriate location on the outside surface of the wall. Similarly, floor and roof sheathing were modeled through the center of joists and rafters, respectively, and displaced to their correct location in the assembly as well. LF plywood was modeled as a single shell element on each surface and assigned its appropriate thickness. Without an established modeling approach for SIPs, they were modeled as two layers of OSB sheathing with thickness assigned, and each layer was offset to its respective location. The shell elements used for the SIPs modeled the two layers of OSB as a single, combined element. The layers of OSB acted integrally together for both in-plane (as shear walls and diaphragms) and out-of-plane loadings on the roof and walls. Buckling of the individual sheets of OSB was not possible in these

shell elements. The expanded polystyrene (isolative foam) was not modeled explicitly; however, its in-plane properties contributing to SIP stiffness have been included through a stiffness calibration with experimental results.

Similar to Pfretzschner et al. (2013), LF plywood sheathing properties, including moduli of elasticity (MOE) and Poisson's ratios for both in-plane and out-of-plane behavior, were calculated using Nairn's (2007) *OSULaminates* software. In-plane and out-of-plane sheathing MOE values for OSB for the TF SIPs were determined based on values provided in the Panel Design Specification (APA Engineered Wood Association 2012). Poisson's ratios assigned to OSB were based on the findings of research performed by Thomas (2003). Stiffness values (G_{12}) for sheathing products were determined by G_{12} calibration, as explained subsequently. Material properties for sheathing elements were assigned as in-plane or out-of-plane values, based on lateral loading direction. For gravity loading only, wall sheathing is considered to act in-plane, and diaphragms (roof and floor) are considered to act out-of-plane.

Framing Connectivity
With the exception of the connections at rafter peaks for the LF structure, all framing connections for both structures were modeled as hinged with moment resistance released in all directions. For the rafter peaks and for gusset plates on the LF, connections were modeled as rigid, restricting rotation in all directions. These assignments reflect the typical assumptions for connection behavior and stiffness.

Sheathing Stiffness Adjustment
To model the in-plane shear stiffness (G_{12}) of shear walls and diaphragms (roof and floor), including effects of edge nail spacing of sheathing, calibrations were performed against known or calculated displacements. The procedure outlined in Pfretzschner et al. (2013), similar to the correlation procedure used by Martin et al. (2011) was used to determine the shear modulus (G_{12}) for the LF plywood sheathing. For each wall, roof, or floor of the LF structure, the G_{12} value for the sheathing material of a simple calibration model created in *SAP2000* was adjusted until its deflection matched that calculated by Eq. C4.3.2-2 in the Wind and Seismic supplement to the NDS (AF&PA 2005b). Calibration models matched the height and length of each TF wall, and one was created for each story of each side wall and gable end. Each model reflected a wall with no openings, sheathed on one side. Framing and sheathing were modeled with identical methods to those presented previously. Material properties for the calibration model matched those for plywood as determined by Nairn's (2007) *OSULaminates* software. Effects of anchor bolts and hold-downs were omitted from these calibrations (and all others)
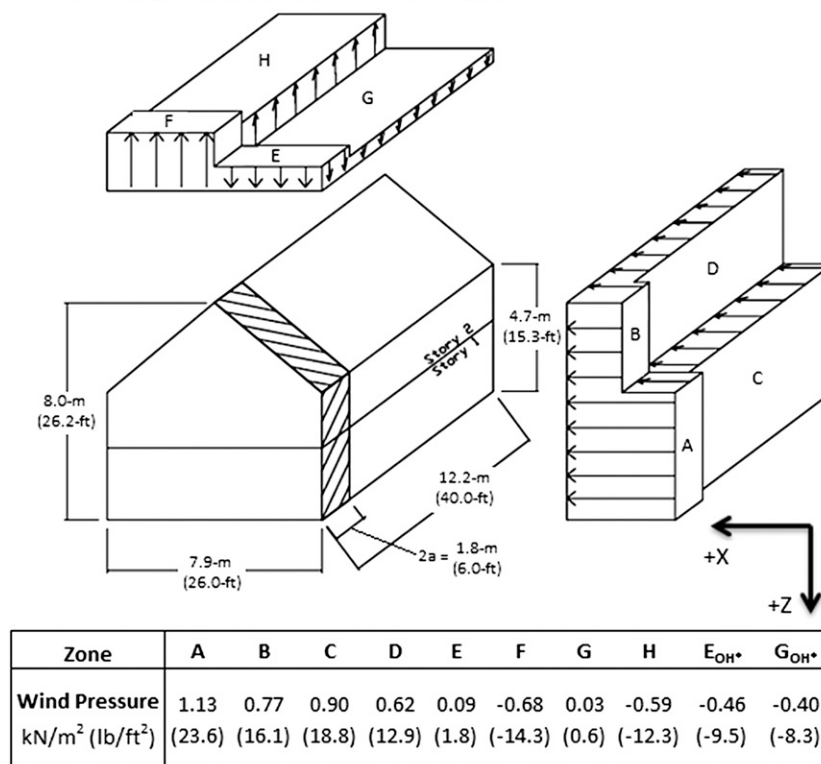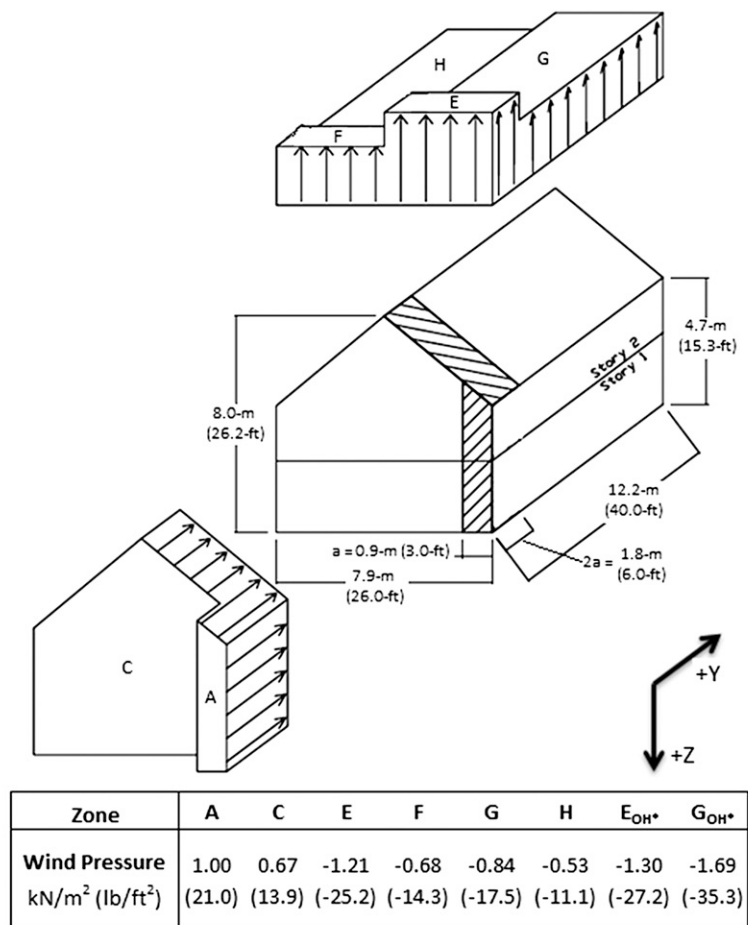
Zone	A	C	E	F	G	H	E_OH*	G_OH*
Wind Pressure kN/m² (lb/ft²)	1.00 (21.0)	0.67 (13.9)	-1.21 (-25.2)	-0.68 (-14.3)	-0.84 (-17.5)	-0.53 (-11.1)	-1.30 (-27.2)	-1.69 (-35.3)

*Overhang wind pressures not shown in figure

Zone	A	B	C	D	E	F	G	H	E_OH*	G_OH*
Wind Pressure kN/m² (lb/ft²)	1.13 (23.6)	0.77 (16.1)	0.90 (18.8)	0.62 (12.9)	0.09 (1.8)	-0.68 (-14.3)	0.03 (0.6)	-0.59 (-12.3)	-0.46 (-9.5)	-0.40 (-8.3)

*Overhang wind pressures not shown in figure

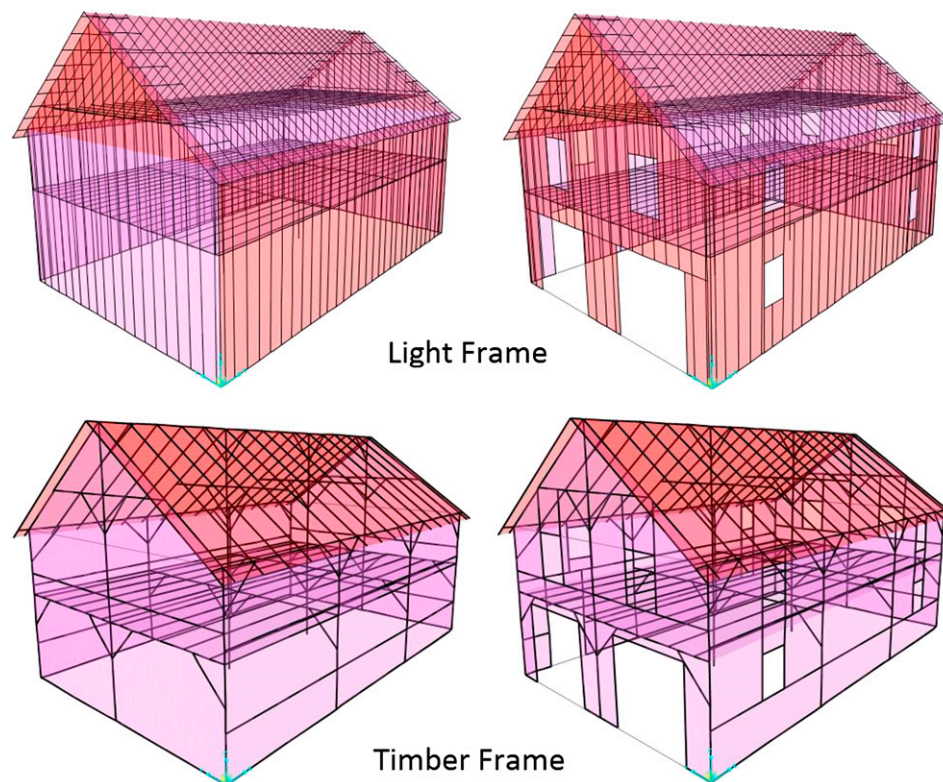**Fig. 2.** General north–south direction wind loading (ASCE 2010, © ASCE)

Fig. 3. LF and TF models, fully enclosed and with openings

by defining all supports in the calibration model as rigid. Foundation connections were incorporated into the structural models themselves, and their effects were modeled conservatively as spring elements. G_{12} values for the LF structure varied based on wall length and height, and varied linearly with length for a given wall height (Pfretzschner et al. 2013).

Because of the limitations of the IRC (ICC 2009), sufficient shear wall area was not available on the gable end of the LF structure due to the garage doors. A portal frame was designed for the necessary lateral force resistance of this wall (Martin et al. 2008). Because of the structural differences and increased stiffness of this moment-resisting frame per unit of sheathing area, a separate stiffness calibration method was necessary. NDS Eq. C4.3.2-2 (AF&PA 2005b) applies only to standard light-framing practices, which do not include the presence of a portal frame. Full-scale testing to determine the deflection and stiffness of a portal frame was performed by Al Mamun et al. (2011). A calibration model was created in *SAP2000* depicting a setup identical to these tests. The G_{12} value of the sheathing elements was then adjusted until deflection results (and therefore stiffness) from testing were matched. Even though the entire portal frame system was modeled, assigning pinned connections to joints allows stiffness to be controlled entirely by sheathing elements. This stiffness value was, therefore, assigned to the shell element material that represents the sheathing on the portal frame.

TF wall and roof sheathing elements were also calibrated against full-scale test results on actual TF elements. TF/SIP wall stiffness was calibrated against stiffness tests performed by Erikson and Schmidt (2003) on a 2-story, 2-bay TF wall section with SIP panels attached. Panel joints coincided with frame members, and wall framing included a sill member, a system of fabrication similar to the TF modeled for this study. A simple calibration model was created in *SAP2000* depicting this identical test setup, and the G_{12} value for the

model sheathing material was adjusted until the deflection from testing was attained by the model. The calibration model was created with two sets of sheathing elements representing the OSB SIP face panels, each offset the appropriate distance from the center line of wall framing. G_{12} values from this calibration procedure were then applied to all TF wall sheathing elements. Roof SIP sheathing stiffness was determined in a similar manner by calibrating against stiffness results from tests performed by Carradine et al. (2004) on a TF roof system sheathed in SIPs.

Wall Anchorage

Similar to Pfretzschner et al. (2013), anchor bolt and hold-down foundation connections were modeled in *SAP2000* with directional linear spring elements. Hold-down connections in the LF were modeled as springs in the vertical (Z) direction only, and anchor bolt connections in both structures were modeled as springs in all three orthogonal directions (X, Y, and Z). Whereas anchor bolts resist uplift, overturning, and horizontal movement, hold-downs were designed to resist uplift only. Axial stiffness of hold-downs (Z-direction) was determined based on properties provided by the manufacturer, Simpson Strong-Tie (Pleasanton, California), and the specific hold-down model selected, model number HDU8-SDS2.5, was based on portal frame design requirements (Simpson Strong-Tie 2013). In accordance with both Martin et al. (2011) and Pfretzschner et al. (2013), axial stiffness of anchor bolts (Z-direction) was based on testing performed by Seaders (2004). Shear stiffness values (X- and Y-directions) were determined in agreement with Martin et al. (2011) using the NDS equation for the load/slip modulus for a dowel-type fastener wood-to-wood connection (AF&PA 2005a). Post bottom connections for the TF were modeled similarly as a linear spring, but with twice the stiffness of a typical anchor bolt (for all three orthogonal directions) since each post bottom connection was performed with two anchor bolts.

Load Path Investigations

Load path investigations applied design loads in ASD loading combinations and observed and compared the relative magnitudes of reactions at each structure's foundation. Specifically, reactions resulting at anchor bolts, hold-downs, and post bottom connections were observed. Additionally, system behavior, most notably member and system deflections, was observed in *SAP2000*. Observations from an initial overall comparison were made based on patterns in load path from gravity loading and resistance to uplift. Additionally, investigations of story drift and twisting, the introduction of large wall openings, a break in load path, and the variation of axial forces in studs and posts, were performed.

TF versus LF Structural Load Path Comparison

Similar to analysis methods used by Pfretzschner et al. (2013), reactions to design loadings were observed at connection points to the foundation. These connections were the anchor bolts and hold-downs for the LF, and post bottoms and anchor bolts for the TF. Each structure therefore had reactions determined along all four walls, as well as at two central locations within the building representing the reactions at the foundation from posts that support second-floor beams in each structural system.

Reactions were represented graphically so that both their magnitude and location were apparent. Comparisons focused on the differences between reactions in TF versus LF without openings for identical loadings, and then similarly across framing systems with openings. Additionally, the effects of introducing openings (doors and windows) on each separate structural system individually were observed. Finally, observations based on the deflected shapes of each structure in *SAP2000* were also made.

Observations were made in an initial comparison between the LF structure and the TF structure (both with and without openings) subject to all load combinations considered. Notable observations further investigated include a variation in pattern of load path between the two structural systems, as well as each structural system's relative resistance to wind-induced uplift.

Story Drift and Gable-End Stiffness

TF construction typically uses vertical posts on exterior walls that span from foundation to roof line. Light framing techniques (platform framing), however, call for a separate stud at each story for exterior walls, introducing a joint at each level. To investigate differences between framing methods with respect to deflection under lateral loads, each standard structure (with openings) was modeled with load combination 5 (dead and wind loads) to observe the maximum effect of north–south wind.

A simultaneous investigation was also performed on the aforementioned structures with the same loading to examine twisting and gable-end stiffness. Where LF design with the IRC required the engineering of a portal frame to sufficiently resist lateral loads, no similar design was added to enhance the stiffness of the gable end with garage doors for the TF. This is because no similar structural element is applicable to or common in TF construction. To compare the stiffness of each gable-end wall with garage doors, load combination 5 with north–south wind loading was applied to each structure.

Large Opening

To compare the effects of introducing large openings in walls for each structural system, large doorways were introduced to the LF and TF models. These additional openings were introduced to the (standard) versions of each structure, already having doors and windows. This was done to mimic the effect of making additional alterations to an actual structure. A large opening was created in the gable end of each structure by removing the wall section between the two garage doors. For the LF, this meant removing several studs and associated sheathing. For the TF, this meant removing one post, as well as its surrounding garage door (small-dimension) framing and associated SIP sheathing. A 140×286-mm (nominal 6×12-in.) header was introduced to the LF, which is the largest typical built-up solid-sawn header available for LF construction. This alteration to the gable end of the LF introduces a clear-span opening of 6.3 m (20 ft 8 in.), which is greater than that allowed by the IRC (ICC 2009) for this header size, but this modification was introduced for comparison purposes in this study only. Similarly, an opening of identical size and position was introduced to the TF. Because of typical timber framing construction methods, no additional framing members (such as a header) were necessary.

A large opening was also introduced to the side of each structure. The size of this opening was dictated by the space available between the two central posts in this wall of the TF. A 140×286-mm (nominal 6×12-in.) header was added above this opening in the LF; however, with a clear span of approximately 4.0 m (13 ft 1 in.), this header is still considered insufficient by the IRC (ICC 2009). As noted previously, this is the largest typical header size available in light framing construction. This large opening has again been introduced for comparison purposes only. Because of typical timber framing construction methods, no additional framing members (such as a header) were added.

Break in Load Path

One of the structural differences between LF and TF is the number of vertical members transmitting loads to the ground. Whereas LF is composed of many small studs, TF relies on a smaller number of larger posts to transmit loads. This applies to rafters and joists as well, and TF simply employs fewer structural framing members. LF, therefore, inherently offers a more redundant design than TF when studs, joists, or rafters are considered, providing more possible load paths to the ground. Thus, it is clear that the omission of one stud in LF would have considerably less effect on load paths than the omission of one post in TF. To investigate the effect of a break in the load path for both structural systems, an investigation was carried out to determine the effect of losing one common member considered critical to each structure, a first-floor central post. The central post furthest from the gable end with garage doors was removed from both the standard TF and the standard LF model.

Post versus Stud Range of Axial Load

Axial loads in the 38×140-mm (nominal 2×6-in.) LF studs and 203×203-mm (8×8-in.) TF posts based on gravity loadings were observed for the range in magnitude. Each structural system was examined fully enclosed, with openings (standard), and with large gable and side openings introduced separately to standard models. Maximum axial forces were observed, and average axial forces were calculated for posts and studs in each model. A value for the ratio of maximum load to the average load was calculated for each, indicating a range in variability of the loads. Load variability between LF studs and TF posts was compared.

Results and Discussion

TF versus LF Structural Load Path Comparison

Patterns in Load Path from Gravity Loading

Results for the magnitudes and locations of base reactions for the structural load paths show a distinctly different pattern for LF and TF. This observation is seen most clearly by considering gravity

loading only (dead, live, and snow loads) with load combination 4. Whereas load transfer to the foundation in the LF shows an even distribution of magnitudes, the TF displays two separate ranges of reaction magnitudes, one at post bottom connections and the other at anchor bolts (where sheathing transmits vertical loads). Fig. 4 shows the foundation connection reactions for the LF structure and the TF structure subject to uniform gravity loads only.

LF reactions range from 9.60 kN (2,150 lbs) to 32.1 kN (7,220 lbs) and show a symmetrical pattern. Load distribution shows a generally higher concentration of reaction at the center of the side walls, and they are reduced as anchor bolt reactions closer to gable-end walls are considered. Load distribution along gable-end walls, however, shows a more consistent magnitude along the length of the wall. These results are in good agreement with patterns observed in a uniform uplift investigation by Pfretzschner et al. (2013), validating correct application of modeling methods.

Load path is inherently dependent on the structural assembly, and a higher concentration of load on the side walls of the LF is because roof loading is transmitted primarily to these walls by rafters. Gable-end walls transmit their own dead load, as well as a small tributary area of roof and a portion of the floor load, each. Central posts support central floor dead and live load only, and show a maximum reaction of 32.1 KN (7,220 lbs) each.

TF foundation reactions from the same load combination show a pattern that is different from the LF structure. Reactions are segregated by magnitude between post bottoms and anchor bolts. As expected, a smaller number of higher-magnitude loads are transmitted to the foundation in TF, as compared with the more uniform distribution observed in the LF assembly. Anchor bolts are located along sill plates that span from one post bottom to the next and serve as connection points for SIP sheathing. Two anchor bolts exist between each post. This allows the sheathing to transmit loads to the foundation. Where post bottom connection reactions show gravity loads transmitted directly by the frame, anchor bolt reactions indicate gravity loads transmitted by SIP sheathing. Although framing members are typically designed to resist 100% of vertical loads, results show that approximately 30% of gravity loads for this assembly have been transmitted to the foundation through the sheathing. Wall post reactions vary owing to structural configuration; however, they are fairly consistent, ranging between 20.0 and 26.3 kN (4,500 and 5,910 lbs). Anchor bolts experience reactions from to 6.17 to 7.13 kN (1,390 to 1,600 lbs). Contrary to LF reactions, higher values here are observed in the gable end of the structure. Because the TF structure uses a ridge beam and central posts that span the height of the floor as well, much of the roof load is transmitted directly to the foundation through this central load path. Whereas the LF structure uses collar ties and rafter ties to transmit roof loads to side walls, the TF configuration creates a load path that does not rely as heavily on side walls. For this reason, the foundation reactions at the central posts in the TF are

approximately 44.8 kN (10,100 lbs), a value 40% higher than the reactions for the LF. Also for this reason, the tapering off of reactions observed in the side walls of LF is not present in TF.

Wind Uplift Resistance

Results for load combination 5, considering the dead load of the structure and wind loading only, reflect the behavior of each structure when additional gravity loads (live and snow) are not present to assist in the resistance of uplift. Fig. 5 shows the results from this loading on both LF and TF considering wind in the general east-west direction. Arrows indicate wind loading direction.

Dark bubble points in Fig. 5 indicate a downward force at the foundation connection (and therefore a positive, upward reaction), and clear bubble points indicate a point of uplift (a negative, downward reaction). At these points, the foundation connections are in compression and tension, respectively. These results show that the windward gable end and the windward side of the LF structure experience uplift along nearly their entire length. Uplift reaction magnitudes are greatest at the windward corner and taper away from this location along both the gable end and side wall.

Where the LF structure exhibits uplift along both windward sides of the building, the TF maintains compressive forces (positive foundation reactions) along both sides, therefore more effectively resisting uplift forces due to wind load. Additionally, foundation connection reactions at post bottom connections continue to be higher in magnitude than anchor bolt connections. This indicates that the lower number of higher-magnitude gravity load reactions more effectively resist uplift.

Because increased gravity loads including dead load are an effective means of resisting uplift, a heavier structure is inherently more likely to maintain compressive (downward) forces along the foundation than a lighter structure, when subjected to wind forces. A sum of the reactions at the foundation indicates that the TF modeled in this study is 32% heavier than the LF. For the purpose of examining the structural effects of the TF composition on uplift resistance without the advantage of increased dead load, a self-weight multiplier was introduced to the load pattern. A self-weight multiplier of 0.76 equates the weight of the TF to the weight of the LF. Fig. 5 indicates the results for foundation reactions for the actual TF subjected to wind and dead load (load combination 5), and Fig. 6 shows these results for the TF structure with a total dead load identical to the LF structure.

Although these results indicate uplift forces at the windward corner of the TF, the region experiencing uplift in this structure is considerably smaller than the uplift seen in the LF under identical loading (Fig. 5). Because the dead load for the TF has been scaled to equal the dead load for the LF, results indicate that the structural configuration of the TF, itself, is more capable of resisting uplift than the structural configuration of the LF.
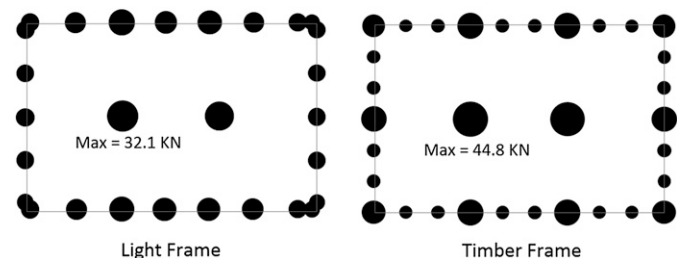

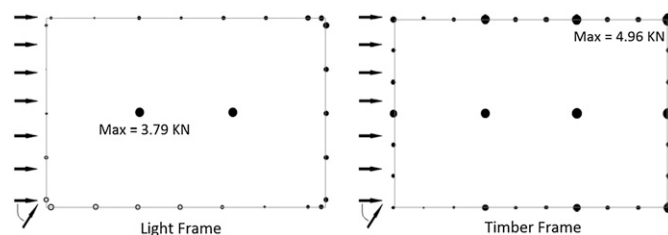**Fig. 4.** Fully enclosed LF and TF foundation reactions, ASD load combination 4

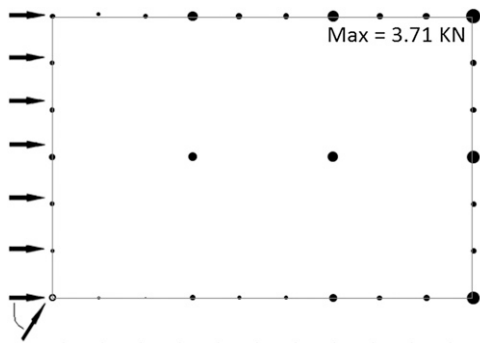**Fig. 5.** Fully enclosed LF and TF foundation reactions, ASD load combination 5

Fig. 6. Fully enclosed TF foundation reactions, equivalent dead load to light-frame, ASD load combination 5
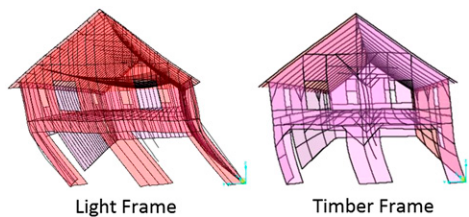

Fig. 7. LF and TF deflection, respectively, standard structures with openings, subjected to north–south wind loading, load combination 5, deflection scale: 200

Fig. 8. LF and TF: effects of gable-end stiffness, load combination 5, north–south wind direction, deflection scale: 200

Fig. 9. LF and TF deflection, respectively, large openings, subjected to gravity loading, load combination 4, deflection scale: 100

Story Drift and Gable-End Stiffness

Deflections observed based on dead and wind loading (load combination 5) considering wind loading from the general north–south direction indicated an increased resistance to story drift in TF compared with LF. Fig. 7 compares the deflection of the TF and LF structures subjected to identical north–south wind loading. Images are viewed at a deflection scale factor of 200 for clarity.

Whereas TF construction often uses continuous posts that span from foundation to roof line, the LF construction method of platform framing introduces a joint at each story. Structures in this study use platform framing because this is the primary method of light framing employed in the United States today (Allen and Thallon 2011). Construction sequence calls for first-floor studs to terminate at a top plate so that the second floor can be installed to serve as a work platform. Installation of the second-floor walls follows. The exterior wall of a typical LF structure, therefore, consists of multiple story-high studs joined vertically at points which essentially act as hinges when subjected to lateral loads (such as wind). [Platform framing replaced balloon framing, a light-framing technique that employs continuous studs for framing exterior walls, in the mid-1950s. Among other deficiencies of balloon framing, it gave way to platform framing because it was more difficult to construct (Allen and Thallon 2011).] The effects of the discontinuous nature of the exterior wall framing in the LF are clear in Fig. 7, where story drift at the center of the north wall at the top of the first floor was approximately 3.5 times greater in LF (10 mm) than in TF (3 mm). All of the deflections given here and subsequently are from a linear elastic model.

Observations between gable ends on the LF and the TF show the effects of gable-end stiffness. Fig. 8 shows the deformations from load combination 5 with a north–south wind direction.

As expected, deflection is 1.5 times greater on the gable end with garage doors (3 mm) than the gable end without these openings (2 mm) on the 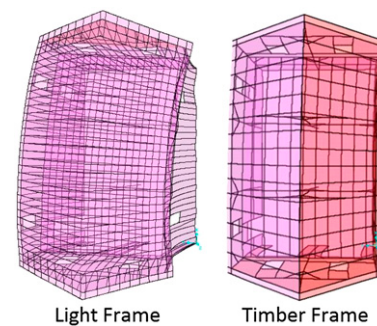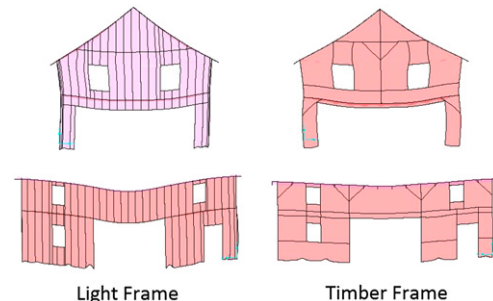TF. Deflections were measured at the floor level of the second story. The LF gable-end wall with garage door openings, however, deflects considerably more than the gable end without openings on the LF (11 versus 5 mm, respectively). For deflection comparison between the two structural systems, the gable end of the LF without garage doors deflected approximately three times further than the similar gable end of the TF. The wall with the garage door in the LF was designed with a moment-resisting frame to increase the stiffness. However, the results show that TF is more resistant to openings introduced in shear walls with respect to lateral stiffness. Although the SIP shear walls carry the majority of the lateral load owing to their stiffness, the knee braces also take a portion of the load. In a complete design of the structure, the braces and joinery connections would need to be addressed as well. The details of these connections have not been included in this study. The deflected shape of the LF also shows more twisting than the TF, both of which use diaphragms considered to be semirigid. Lateral loads are transmitted to shear walls in rigid (or semirigid) diaphragm structures to reflect the stiffness of each shear wall, and therefore twisting occurs in the LF structure because the stiffness of the portal frame is less than the stiffness of the opposing gable-end shear wall. A stiffer portal frame would, therefore, be required to mitigate LF twisting. It is important to note that for all results based on loads applied laterally to the TF structure, lateral behavior is dictated by the stiffness of sheathing.

Large Opening

Effects of introducing large openings in the gable end and side of each structure were investigated. Load combination 4 (gravity loads only) was applied to the TF and LF structures with each large opening. Vertical deflections at the top of the opening are 3 mm for the LF with a large opening on the gable end and 9 mm for a large opening on the side of the structure. For the TF, the deflections are 4 and 3 mm, for large openings on the gable end and side, respectively. Fig. 9 shows

the deformed shape of the gable end and side of each structure at a deflection scale factor of 100.

TF load paths appear to adapt easily to the presence of a large opening in the side of the structure. This is attributed to the smaller-magnitude loads transmitted by the sheathing removed to create the opening. Because gravity load paths in the TF structure rely primarily on posts for transmission to the foundation, and post locations have not been altered to include the opening, little change in load path is observed. The LF structure, however, experiences considerable deflection in the header above the opening, as well as in the eave line of the roof. Change in load path within the LF structure due to a large opening in the side of the structure relies on the header, installed above the opening, to transmit loads to adjacent studs. Additionally, the location of this opening is where the magnitudes of loads transmitted by the side wall are the greatest (Fig. 5). This supports the conclusion that a TF structure is more resistant to the introduction of large openings than LF, provided posts are unaltered and available for load transmission. Thus, it is preferable to locate a large opening in a gable end rather than the side of an LF. This conclusion is in agreement with the findings of Martin et al. (2011) and Pfretzschner et al. (2013).

The only post removed for the investigation involving large openings was a central gable-end post. The joists are framed directly into a beam above this post that spans the complete width of the building. Loads carried by the joists are therefore transmitted along this beam to other posts.

Break in Load Path

Fig. 10 shows the resulting deflection in floor systems for the LF and the TF when a first-floor central post is removed. Even though the removed central post in the TF supports additional roof load (the first-floor central post in the LF does not support roof load), the TF floor system deflects only approximately 25% as much as the LF floor system (6 versus 22 mm, respectively). The TF is, therefore, less sensitive to this break in load path than the LF. The internal column was included in both TF and LF for comparison purposes with the specific, actual structure being examined, however, in most LF structures, interior load-bearing walls would be present instead and provide additional structural redundancy. Also, material and
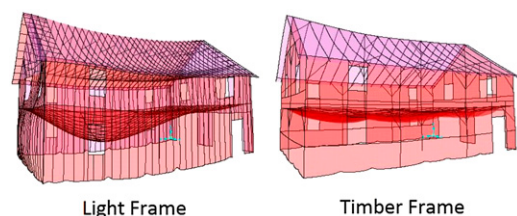

Light Frame   Timber Frame

Fig. 10. Break in load path, deflection from central post removal from LF and TF, deflection scale: 100

construction uncertainties have not been modeled in the study, so their effects on safety are not included.

Post versus Stud Range of Axial Load

Table 2 shows maximum axial loads in the LF studs and TF posts as well as average loads based on gravity loading only (load combination 4). The maximum load shown is the greatest single axial force in a stud for the LF and the greatest single axial force in a post for the TF. The averages are over all of the single studs or posts in the structures, respectively. When the maximum is considerably higher than the average, the actual factor of safety is diminished owing to the concentration of loadings. TF posts consistently show a maximum-to-average axial load ratio of approximately 2.0 for all structural options examined. The LF, however, shows an increase in load variability as the frame complexity increases and openings are introduced. Although the ratio of maximum load divided by average load is only 1.43 for the fully enclosed LF, the ratio increases to 3.72 for the LF with a large side opening. Although a factor of safety is applied during design to typical structural, variability reduces the actual effective factor of safety. TF posts must be designed to withstand at least two times the average load expected. LF studs, however, must be designed to carry significantly more because of even greater variability of loads in some cases.

Conclusions

Structural models of a TF and LF structure were created in *SAP2000* using modeling methods developed by Martin et al. (2011) and Pfretzschner et al. (2013). Comparisons were made between structural systems (with and without openings) based on the behavior of each model under gravity and wind loads. Results were based on reaction forces at the foundation in each structure, as well as observed deflections of members and assemblies. Specifically, observations of reaction patterns from gravity loading, as well as uplift resistance from wind loading, were made. Additional investigations performed included observing story drift and twist, introducing large wall openings, a break in load path, and observing the range of axial loads in TF posts and LF studs.

Results show that the TF structure outperforms the LF structure in many aspects. TFs more effectively resist uplift with fewer, more heavily (gravity) loaded posts. Story drift and twisting were also more effectively resisted by the TF, because of continuous posts resisting out-of-plane wind loading more effectively than platform-framed exterior walls, and because of the greater stiffness of the SIP panels compared with the LF shear walls. Additionally, TFs are more suitable for the addition of large openings in the side of a structure provided these openings are introduced in between posts. Whereas the LF in this study relies on side walls (perpendicular to the rafter direction) for the primary transmission of roof loads, the TF uses central posts that carry a large percentage of gravity loads through the center of the structure. Based on observations of axial

Table 2. Axial Load Distribution in LF Studs and TF Posts

Structural composition	LF studs 38 × 140 mm (2 × 6 in.)			TF posts 203 × 203 mm (8 × 8 in.)		
	Maximum axial load, kN (lbs)	Average axial load, kN (lbs)	Maximum/average	Maximum axial load, kN (lbs)	Average axial load, kN (lbs)	Maximum/average
Fully enclosed	4.54 (1,020)	3.15 (709)	1.44	71.2 (16,003)	35.6 (7,993)	2.00
Standard (with openings)	5.23 (1,175)	3.13 (704)	1.67	70.7 (15,905)	36.2 (8,140)	1.95
Large gable-end opening	6.30 (1,416)	3.14 (705)	2.00	76.6 (17,226)	37.8 (8,493)	2.03
Large side opening	11.93 (2,681)	3.21 (721)	3.72	71.0 (15,962)	34.9 (7,836)	2.04

loads in studs and posts in variations of the models, the range of loads is smaller in TF members.

It should be recognized that the structural modeling described here is for a limited scope of building configurations. Future studies should examine a wider range of buildings that include interior walls and irregular shapes. Other areas for further study include a thorough cost analysis and comparison for different types of construction as well as inclusion of commonly used metal-plate-connected trusses for LF. Much research has already been performed on design and analysis of trusses, for example, Mtenga et al. (1995) and Cramer et al. (2000), so the groundwork for modeling of these trusses, including variability in performance, is well established.

References

Allen, E., and Thallon, R. (2011). *Fundamentals of residential construction*, 3rd Ed., Wiley, Hoboken, NJ.

Al Mamun, A., Ghasan, D., Ni, C., Mohammad, M., Chui, Y. H., and Asiz, A. (2011). "Alternative bracing systems in light-wood frame buildings." *Proc., Canadian Society for Civil Engineering 2011 General Conf.,* Montréal.

American Forest and Paper Association (AF&PA). (2005a). "National design specification for wood construction (NDS)." American National Standards Institute/American Forest and Paper Association (ANSI/AF&PA), Washington, DC.

American Forest and Paper Association (AF&PA). (2005b). "Special design provisions for wind and seismic." American National Standards Institute/American Forest and Paper Association (ANSI/AF&PA), Washington, DC.

APA Engineered Wood Association. (2012). *Panel design specification*, Tacoma, WA.

ASCE. (2010). "Minimum design loads for buildings and other structures." *ASCE/SEI 7-10*, Reston, VA.

Bulleit, W. M., Sandberg, B. L., Drewek, M. W., and O'Bryant, T. L. (1999). "Behavior and modeling of wood-pegged TFs." *J. Struct. Eng.*, 10.1061/(ASCE)0733-9445(1999)125:1(3), 3–9.

Carradine, D. M., Woeste, F. E., Dolan, J. D., and Loferski, J. R. (2004). "Utilizing diaphragm action for wind load design of TF and structural insulated panel buildings." *For. Prod. J.*, 54(5), 73–80.

Computers and Structures. (2012). *CSI analysis reference manual: For SAP2000, ETABS and SAFE*, Berkeley, CA.

Cramer, S. M., Drozdek, J. M., and Wolfe, R. W. (2000). "Load sharing effects in light-frame wood-truss assemblies." *J. Struct. Eng.*, 10.1061/(ASCE)0733-9445(2000)126:12(1388), 1388–1394.

Doudak, G. (2005). "Field determination and modeling of load paths in wood light-frame structures." Ph.D. thesis, McGill Univ., Montréal.

Erikson, R. G., and Schmidt, R. J. (2003). "Behavior of traditional TF structures subjected to lateral load." Ph.D. thesis, Univ. of Wyoming, Laramie, WY.

Google Sketch-Up Pro 8.0.15158 [Computer software]. Mountain View, CA, Google.

International Code Council (ICC). (2009). *International residential code for one- and two-family dwellings – 2009*, Country Club Hills, IL.

Malone, B. P. (2013). "LF versus traditional TF: A study in comparing the differences." M.S. thesis, Oregon State Univ., Corvallis, OR.

Martin, K. G., Gupta, R., Prevatt, D. O., Datin, P., and van de Lindt, J. (2011). "Modeling system effects and structural load paths in a wood-framed structure." *J. Archit. Eng.*, 10.1061/(ASCE)AE.1943-5568.0000045, 134–143.

Martin, Z., Skaggs, T.D., Keith, E.L., and Yeh, B. (2008). "Principles of mechanics model for wood structural panel portal frames." *Proc., Structures Congress 2008*, D. Anderson, C. Ventura, D. Harvey, M. Hoit, eds., ASCE, Reston, VA, 1–9.

Mtenga, P. V., Cramer, S. M., Peyrot, A. H., and Wolfe, R. W. (1995). "System factors for light-frame wood truss assemblies." *J. Struct. Eng.*, 10.1061/(ASCE)0733-9445(1995)121:2(290), 290–300.

Nairn, J. (2007). *OSULaminates – Java application for laminated theory analysis, version 2.1,* ⟨http://www.cof.orst.edu/cof/wse/faculty/Nairn/OSULaminates.html⟩ (Feb. 1, 2013).

Pfretzschner, K., Gupta, R., and Miller, T. H. (2013). "Practical modeling for load paths in a realistic, LF wood house." *J. Perform. Constr. Facil.*, in press.

Prevatt, D. O., et al. (2012). "Building damage observations and EF classifications from the Tuscaloosa, AL and Joplin, MO tornadoes." *Proc., Structures Congress 2012,* ASCE, Reston, VA, 999–1010.

SAP 2000 [Computer software]. Walnut Creek, CA, Computers and Structures.

Seaders, P. (2004). "Performance of partially and fully anchored wood frame shear walls under monotonic, cyclic and earthquake loads." M.S. thesis, Oregon State Univ., Corvallis, OR.

Shanks, J., and Walker, P. (2009). "Strength and stiffness of all-timber pegged connections." *J. Mater. Civ. Eng.*, 10.1061/(ASCE)0899-1561(2009)21:1(10), 10–18.

Simpson Strong-Tie. (2013) "LTT/HTT tension ties." ⟨http://www.strongtie.com/products/connectors/HDU-DTT2.asp⟩ (May 5, 2013).

TF Engineering Council (TFEC). (2010). *Standard for design of TF structures and commentary*, TF Engineering Council, Becket, MA.

Thomas, W. H. (2003). "Poisson's ratios of an oriented strand board." *Wood Sci. Technol.*, 37(3–4), 259–268.

van de Lindt, J. W., Graettinger, A., Gupta, R., Skaggs, T., Pryor, S., and Fridley, K. (2007). "Performance of wood-frame structures during Hurricane Katrina." *J. Perform. Constr. Facil.*, 10.1061/(ASCE)0887-3828(2007)21:2(108), 108–116.